

9. V. I. Polezhaev, "Convective interaction in a cylindrical vessel partially filled with liquid, with heat supplied to the side and free surfaces and to the base," *Izv. Akad. Nauk SSSR, Mekh. Zhidk. Gaza*, No. 4, 77-88 (1972).

METHODS OF SOLVING CONVECTION AND HEAT-TRANSFER PROBLEMS IN  
REGIONS WITH BOUNDARIES THAT VARY IN FORM OVER TIME

A. P. Ezerskii

UDC 532.516

A method of numerical solution of nonsteady two-dimensional Navier-Stokes equations in regions with curvilinear moving boundaries is proposed. As an example, the solution of the problem of melting with convection in the liquid phase is presented.

The need to investigate convective problems in regions of complex geometry has given rise to a stream of new numerical methods of calculation. At the same time, the question of the accuracy of these methods, the minimal calculation time, and the demands which they make remains to be resolved. For nonsteady problems with varying geometry of the region, the calculation time is one of the basic factors in selecting the numerical integration scheme.

Two approaches to the solution of this kind of problem exist: the first is associated with the interpolation of the boundary positions with respect to the points of the calculation grid and the second with matching the grid lines with the boundaries. As shown in [1], because of the large rounding errors associated with the presence of grid points very close to the boundary, it is preferable to use the second approach, the more so in that in this case the specification of the boundary conditions is considerably simplified.

A general description of the method of coordinate transformation for conservative and nonconservative systems of partial differential equations of first and second order was given in [2]. This method was developed in [3] for the problem of heat conduction with a single mobile boundary. Extensive results on the use of the method of automatic numerical construction of a curvilinear coordinate system of general form with grid lines coinciding with all the boundaries of a body of arbitrary form were published in [4]. Because of its generality, this approach is especially applicable. However, in the case when the boundaries of the region change form, additional iterations are necessary at each computational step to reconstruct the coordinate system, which may lead to significant increase in the time (i.e., cost) of the calculations.

In the present work, a simple numerical method of solving nonsteady heat- and mass-transfer problems in regions with moving curvilinear boundaries is proposed, on the basis of transforming the physical region to rectangular form. This transformation is not associated with the solution of a system of Poisson equations for the coordinates, i.e., does not require additional consumption of computer resources.

Consider a physical region consisting in the general case of our moving curvilinear boundaries (Fig. 1). The corresponding transformed region will have fixed rectilinear boundaries. The coordinate-transformation law is determined in the form

$$\xi = \frac{x - x_1}{x_2 - x_1}, \quad \eta = \frac{y - y_1}{y_2 - y_1}, \quad \tau = (\text{const})t, \quad (1)$$

where

$$\begin{aligned} x_1 &= x_1(y, t), & x_2 &= x_2(y, t), \\ y_1 &= y_1(x, t), & y_2 &= y_2(x, t), \end{aligned} \quad (2)$$

and therefore

$$\xi = \xi(x, y, t), \quad \eta = \eta(x, y, t). \quad (3)$$

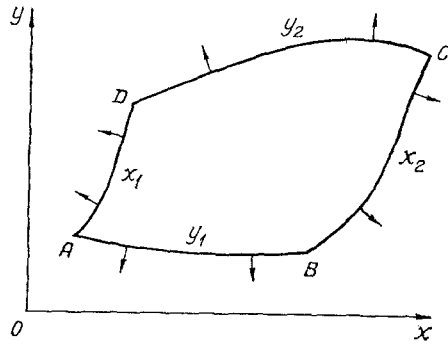


Fig. 1. Diagram of the physical region with moving curvilinear boundaries.

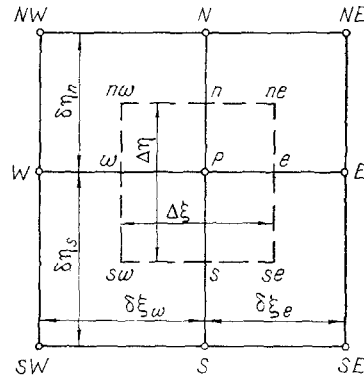


Fig. 2. Diagram of the control volume.

In most practical cases, the boundary coordinates  $x_1$ ,  $x_2$ ,  $y_1$ ,  $y_2$  are known in advance; however, as a rule, they are found to be in a functional dependence on the field variables (for examples, temperatures or pressures) and hence may be determined in the course of calculation. The elucidation of this dependence is sometimes an independent problem, requiring both theoretical and experimental study.

Nevertheless, for a series of phenomena, this functional dependence may readily be formulated on the basis of the balance relations at the boundary. Thus, for a large class of problems with the presence of phase transition — known as problems with mobile boundaries in the literature [3] — the position of an individual boundary (for example,  $x_2$  in Fig. 1) may be determined from the energy balance at this boundary. Assuming that all the heat supplied from the internal phase is absorbed on account of the latent heat of phase transition, the following expression may be written

$$-\lambda \frac{\partial T}{\partial n} = \rho L \left. \frac{\partial x_2}{\partial t} \right|_n \quad (4)$$

Thus, the position of the necessary boundary becomes unknown immediately after calculation in each time layer of the temperature field.

The initial positions of the boundaries  $x_1(y, t_0)$  and so on required for the calculation, like the initial distribution of field variables for the nonsteady problem, are either specified or are determined on the basis of simplified models or using a preliminary approximate series of calculations.

To write the transfer equations, consider any incompressible liquid conforming to the Boussinesq approximation. For a Cartesian coordinate system, these equations may be generalized by the following dependence

$$\varepsilon(\Phi_t - \psi_y \Phi_x + \psi_x \Phi_y) = \Gamma(\Phi_{xx} + \Phi_{yy}) + S, \quad (5)$$

where  $\varepsilon = 0$  for the Poisson equation and  $\varepsilon = 1$  in other cases.

Replacing the derivatives with respect to  $x$ ,  $y$ ,  $t$  by the derivatives with respect to  $\xi$ ,  $\eta$ ,  $\tau$  in Eq. (5) in accordance with the rules of differentiation of complex functions, and regrouping the terms, the following equation is obtained, reflecting the distribution of over the transformed region

$$\varepsilon \tau_t \Phi_\tau + u \Phi_\xi + v \Phi_\eta = \Gamma[(\alpha \Phi_\xi)_\xi + 2\beta \Phi_{\xi\eta} + (\gamma \Phi_\eta)_\eta] + S', \quad (6)$$

where

$$\begin{aligned} u &= -\varepsilon J \psi_\eta + \varepsilon \xi_t - \Gamma P; & v &= \varepsilon J \psi_\xi + \varepsilon \eta_t - \Gamma Q; \\ J &= \xi_x \eta_y - \xi_y \eta_x; & \alpha &= \xi_x^2 + \xi_y^2; & \beta &= \xi_x \eta_x + \xi_y \eta_y; & \gamma &= \eta_x^2 + \eta_y^2; \\ P &= \xi_{xx} + \xi_{yy} - \alpha_\xi; & Q &= \eta_{xx} + \eta_{yy} - \gamma_\eta. \end{aligned}$$

The control-volume (CV) method is proposed for the approximation of Eq. (6); it has two features favorably distinguishing it from other finite-difference methods: on the one hand, it allows the terms arising as a result of transformation to be easily interpreted; on the other, it ensures the general property of conservation.

After simple transformations, the result obtained after integrating Eq. (6) over the CV (Fig. 2) with the corresponding assumptions [5] is

$$a_P \Phi_P = a_E \Phi_E + a_W \Phi_W + a_N \Phi_N + a_S \Phi_S + D_P (\Phi_{NE} - \Phi_{SE} - \Phi_{NW} + \Phi_{SW}) + b_P, \quad (7)$$

where

$$\begin{aligned} a_P^0 &= \varepsilon \tau_t \Delta \xi \Delta \eta / \Delta \tau; & b_P &= a_P^0 \Phi_P^0 + S'_C \Delta \xi \Delta \eta; \\ a_P &= a_E + a_W + a_N + a_S + a_P^0 - S'_P \Delta \xi \Delta \eta; & D_P &= \Gamma \beta_P / 2; \\ a_E &= D_E + \max\{-C_E, 0\}; & a_W &= D_W + \max\{C_W, 0\}; \\ a_N &= D_N + \max\{-C_N, 0\}; & a_S &= D_S + \max\{C_S, 0\}; \\ D_E &= \Gamma \alpha_e \Delta \eta / \delta \xi_e; & D_W &= \Gamma \alpha_w \Delta \eta / \delta \xi_w; \\ D_N &= \Gamma \gamma_n \Delta \xi / \delta \eta_n; & D_S &= \Gamma \gamma_s \Delta \xi / \delta \eta_s; \\ C_E &= -\varepsilon J_e (\psi_{NE} + \psi_N - \psi_{SE} - \psi_S) / 4 + (\varepsilon \xi_t - \Gamma P)_e \Delta \eta; \\ C_W &= -\varepsilon J_w (\psi_{NW} + \psi_N - \psi_{SW} - \psi_S) / 4 + (\varepsilon \xi_t - \Gamma P)_w \Delta \eta; \\ C_N &= \varepsilon J_n (\psi_{NE} + \psi_E - \psi_{NW} - \psi_W) / 4 + (\varepsilon \eta_t - \Gamma Q)_n \Delta \xi; \\ C_S &= \varepsilon J_s (\psi_{SE} + \psi_E - \psi_{SW} - \psi_W) / 4 + (\varepsilon \eta_t - \Gamma Q)_s \Delta \xi. \end{aligned}$$

If Eq. (6) is written in form after integration, the physical meaning of the coefficients appearing there is easily interpreted. Thus,  $\Gamma \alpha$ ,  $\Gamma \beta$ ,  $\Gamma \gamma$ , appearing in the diffusional terms  $D$ , characterize the intensity of diffusional transfer in the corresponding directions. The Jacobian  $J$  regulates the attenuation or amplification of the convective currents in the transferred CV cell. The derivatives  $\xi_t$  and  $\eta_t$  may be interpreted as pseudoconvection due to motion of the corresponding CV boundaries and the coefficients  $P$  and  $Q$  as pseudoconvection on account of distortion of the CV boundaries.

Note that the coefficients  $\alpha$  are always positive (a consequence of the application of the "counterflow" scheme), and therefore the static instability characteristic of schemes with central differences does not appear. This is the basic reason for considering all the coefficients on  $\Phi_\xi$  and  $\Phi_\eta$  as convective components.

The use of a so-called exponential scheme obtained from the accurate solution for one-dimensional steady convection was proposed in [5] in order to obtain more accurate expression for the coefficients  $\alpha$ . With the aim of economizing on machine time, the use of the following approximate function is recommended

$$A(R) = \max\{0, (1 - 0.1|R|)^3\}. \quad (8)$$

The coefficients  $\alpha$  should take the following form here:

$$a_i = D_i A(C_i / D_i) + \max\{\mp C_i, 0\}, \quad i = E, N, W, S. \quad (9)$$

The use of Eqs. (8) and (9) indicates that, at large convective fluxes, the influence of diffusion is negligible. With commensurate magnitudes of the convection and diffusion, the contribution of the diffusional term decreases, which leads to attenuation of the influence of numerical (spurious) diffusion. The influence of introducing this scheme is discussed below.

Two more satisfactory schemes may be used to solve Eq. (7): the alternating-direction method and the successive-relaxation method. In the first case, Eq. (7) breaks down to two forms of equations, which are solved by the fitting method [1]

$$-a_E \Phi_E^I + a_P \Phi_P^I - a_W \Phi_W^I = B_1, \quad -a_N \Phi_N^{II} + a_P \Phi_P^{II} - a_S \Phi_S^{II} = B_2, \quad (10)$$

where I and II are the first and second directions of fitting. In the second case, with the chosen relaxation factor  $\omega$  [1], after determining  $\Phi_P^*$  directly from Eq. (7) at each point of the calculation grid, relaxation occurs

$$\Phi_P^{(k+1)} = \omega \Phi_P^* + (1 - \omega) \Phi_P^{(k)}. \quad (11)$$

Boundary conditions must be considered to close the system of equations.

Hydrodynamic boundary conditions are specified using vortices and current functions. The value of the current function at the boundary is determined by numerical integration of the velocity profile through the given physical boundary (for example, the velocity  $v_b$  through AB in Fig. 1)

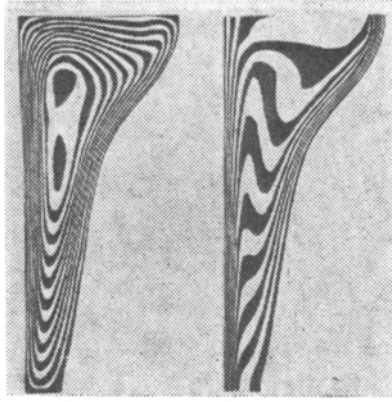


Fig. 3

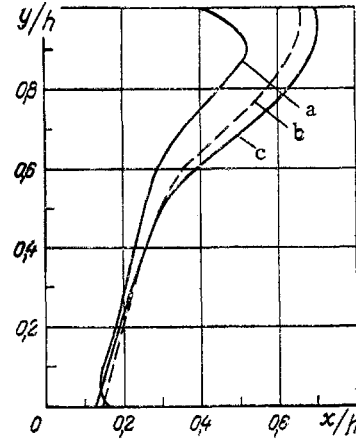


Fig. 4

Fig. 3. Pattern of current lines and isotherms in the melt obtained using a special graph-plotting program employing linear interpolation;  $\tau = 0.02$ .

Fig. 4. Comparison of the phase-boundary positions calculated using various methods;  $\tau = 0.03$ .

$$\psi_b = \int_A^x v_b ds. \quad (12)$$

With motion of the boundary AB at the velocity  $u_b$ , the current function is expediently expressed in the hypothetical layer  $b - 1$  adjacent to the boundary

$$\psi_{b-1} = \psi_{b+1} - 2u_b \Delta n. \quad (13)$$

If the condition of slip or symmetry is specified, the corresponding expression for the current function is

$$\psi_{b-1} = 2\psi_b - \psi_{b+1}. \quad (14)$$

After determining the current function at internal points, at the boundaries, and in the hypothetical layer, the vortices at the boundaries may be calculated from a finite-difference analog of the expression

$$\zeta_b = \frac{\partial^2 \psi}{\partial n^2} \Big|_b + \frac{\partial^2 \psi}{\partial s^2} \Big|_b. \quad (15)$$

The boundary conditions for the other variables may be generalized by the dependence

$$p_1 \Phi_b + p_2 \frac{\partial \Phi}{\partial n} \Big|_b = q, \quad (16)$$

where  $p$  and  $q$  are the specified constants, which may depend on  $x$ ,  $y$ ,  $t$ . These aspects of the numerical boundary conditions were outlined in [1].

As an illustration of the use of the given method, consider free convection in the melting of a solid at the melting point around an isothermal vertical wall of height  $h$ . The density of the two phases is assumed to be the same; the liquid phase conforms to the Boussinesq approximation with a constant volume expansion coefficient. The end walls are adiabatic. The coordinates of the boundary (Fig. 1) are specified in the form  $y_1 = 0$ ,  $y_2 = h$ ,  $x_1 = 0$ ,  $x_2 = x_f(y, t)$ . Transformation of Eq. (1) leads to the relations

$$\xi = \frac{x}{x_f(y, t)}, \quad \eta = \frac{y}{h}, \quad \tau = \text{FoSte}. \quad (17)$$

Introducing the Stefan number in dimensionless time allows the parametric dependence on the latter to be reduced [6]. The form of the equations describing the process in the physical region and the introduction of dimensionless parameters may be found in [6, 7].

Numerical calculation was performed on the basis of the Fortran program CONFIX developed at the Moscow Power Institute in the Department of Heat- and Mass-Transfer Processes and

Apparatus. The sequence of calculation includes the following stages: 1) A  $\xi$ - $\eta$  finite-difference grid is constructed; the initial values for the vortices and the current function are taken to be zero over the whole region, and the initial thickness of the melt is specified, so as to avoid unnecessary calculations, from the condition that free convection has no influence. Here  $\tau_0$  and the initial temperature distribution are determined on the basis of the classical Stefan solution [8]. 2) In the new time layer, the values of the coordination-transformation coefficients are determined on the basis of Eq. (17). 3) The successive-relaxation method is used to solve Eq. (7) for dimensionless values of the vortex, the current function, and the temperature. The relaxation factors are 1, 1.5, and 1. The error in all the variables is held less than 1%. 4) The values of the vortex are calculated on the basis of the condition of adhesion at all the boundaries and the temperature condition at the adiabatic ends. The position of the phase-boundary coordinates is determined as a result of integrating the heat-flux balance equation - Eq. (4) - at the phase boundary

$$(x_f/h) = \sqrt{(x_f^0/h)^2 + 2\Delta\tau(-\theta_g)[1 + (x_f^0)_y^2]}. \quad (18)$$

5) Steps 2-4 are repeated until the required time step is reached.

A uniform  $11 \times 21$  grid was most successfully used; this is explained by the smooth variation in the melt thickness over the height. The time step was  $5 \cdot 10^{-5}$ . The calculation time on an ES-1033 computer was 40-50 min, on average.

Some results of the calculation for  $Ra = 4.5 \cdot 10^6$ ,  $Ste = 1$ ,  $Pr = 1$  are shown in Figs. 3 and 4. A general idea of the character of flow and heat transfer at some moment of time may be obtained by considering Fig. 3. In the present model, it is assumed that the density of the liquid phase decreases with increase in temperature. This leads to upward displacement of the heated liquid layers along the warming plate, thereby resulting in a greater melting rate in the upper part of the region. This isotherm pattern shows in which zones large temperature gradients must be expected. This is in complete agreement with the interference diagrams obtained from experiments with the melting of paraffin [9]. The theoretical phase-boundary positions are compared in Fig. 4. Curve *a* corresponds to [6], where a simplified method was used: in particular, no account was taken of the derivatives  $(x_f)_y$ ,  $(x_f)_{yy}$ . The characteristic deviations of the phase boundary from the normal close to the ends are associated with the introduction of a hypothetical grid layer for the calculation of the temperature at the adiabatic ends, which leads to additionally taking account of the wall heat conduction. Curves *b* and *c* correspond to the present work; curve *b* is characterized by the use of Eq. (7) and curve *c* to the use of Eqs. (8) and (9) additionally. Thus, the introduction of the refining coefficients  $A(R)$  in the calculation is equivalent to relative increase in the contribution of the convective components, as would be expected.

#### NOTATION

$x, y, t$ , physical coordinates;  $\xi, \eta, \tau$ , transformed coordinates;  $\lambda$ , thermal conductivity;  $T$ , temperature;  $n$ , normal to boundary;  $\rho$ , density;  $L$ , heat of phase transition;  $\Phi$ , generalized dependent variable;  $\psi$ , current function;  $\zeta$ , vortex;  $\Gamma$ , generalized diffusion-transfer coefficient;  $S = S_c + S_p\Phi$ , source term;  $S'$ , transformed source term;  $J, \alpha, \beta, \gamma, P, Q$ , transformation coefficients;  $C_i, D_i$ , convective and diffusional components of the finite-difference equation;  $R_i = C_i/D_i$ ;  $\omega$ , relaxational factor;  $ds, \partial s$ , elementary area at boundary;  $h$ , height of warming wall;  $x_f$ , coordinate of phase boundary;  $\theta$ , dimensionless temperature;  $Fo = \hat{a}t/h^2$ ,  $Ste = c\Delta T/L$ ,  $Ra = g\hat{\beta}\Delta Th^3/\nu\hat{a}$ ,  $Pr = \nu/\hat{a}$ , Fourier, Stefan, Rayleigh, and Prandtl numbers;  $\hat{a}$ , thermal diffusivity;  $c$ , specific heat;  $\Delta T$ , difference between wall temperature and melting point;  $g$ , acceleration due to gravity;  $\hat{\beta}$ , temperature-expansion coefficient;  $\nu$ , kinematic viscosity. Indices:  $n, s, e, w, N, S, E, W, P, CV$  elements (Fig. 2);  $x, y, t, \xi, \eta, \tau$ , differentiation with respect to the given variable;  $b$ , relation to the grid point at the boundary;  $0$ , initial; superscripts;  $0$ , relation to the previous time layer;  $k$ , iteration number.

#### LITERATURE CITED

1. P. J. Roache, *Computational Fluid Dynamics*, Hermosa (1976).
2. W. L. Obercampf, "Domain mapping for the numerical solution of partial differential equations," *Int. J. Num. Meth. Eng.*, 10, 211-223 (1976).
3. C. Hsu, E. M. Sparrow, and S. V. Patancar, "Numerical solution of moving boundary problems by boundary immobilization and a control-volume-based finite-difference scheme," *Int. J. Heat Mass Transfer*, 24, 1335-1343 (1981).

4. J. F. Thompson, F. G. Thames, and C. W. Mastin, "TOMCAT: A code for numerical generation of a boundary-fitted curvilinear coordinate system on fields containing any number of arbitrary two-dimensional bodies," *J. Comp. Phys.*, 24, 274-302 (1977).
5. V. S. Patancar, *Numerical Heat Transfer and Fluid Flow*, Hemisphere, Washington, DC (1980).
6. V. V. Galaktionov and A. P. Ezerskii, *Analysis of Melting, Taking Account of Free Convection* [in Russian], Paper No. 5606-82 Deposited at VINITI (1982).
7. V. V. Galaktionov, A. P. Ezerskii, and I. N. Zhukova, "Melting in the presence of free convection in a melt," in: *Scientific Proceedings of the Moscow Power Institute* [in Russian], No. 560 (1982), pp. 27-35.
8. A. V. Lykov, *Theory of Heat Conduction* [in Russian], Vysshaya Shkola, Moscow (1967).
9. P. D. Van Buren and R. Viskanta, "Interferometric measurement of heat transfer during melting from a vertical surface," *Int. J. Heat Mass Transfer*, 23, 568-571 (1980).

#### HYDRODYNAMIC INSTABILITY AND REGIMES OF FRAGMENTATION OF DROPS

A. G. Girin

UDC 532.529.6

Estimates of the dispersal parameters are obtained and an explanation is proposed for the mechanism of various types of destruction on the basis of a linear analysis of the stability of the surface of a drop.

The fragmentation of liquid drops and jets by a high-speed gas stream is an important process in many industrial installations and can exert considerable influence on the flow of gas-drop mixtures. Because of the complexity of the physical phenomena comprising this process, fragmentation is studied predominantly by empirical methods, so that it has been well investigated experimentally but a complete theoretical model does not yet exist [1, 2], preventing one from obtaining reliable estimates of the sizes of the droplets torn off and the time of their separation and clarifying the various types of destruction.

In [3] an attempt was made to give a unified explanation of fragmentation as the manifestation of hydrodynamic instability of the drop surface. In that paper a mathematical model of a fragmenting drop was constructed on the basis of a solution of the problem of the stability of an accelerated tangential velocity discontinuity, and it was concluded that the description of the phenomenon is adequate, despite the definite quantitative inconsistency.

Further refinement of the model, connected with an investigation of the inviscid instability of the interface between two media with the property of continuity of the velocity profile inherent to actual fluxes, showed [4] that the model of a tangential discontinuity can only serve as a rough approximation, since the decrease in the velocities of the media in the boundary layers has a considerable stabilizing action.

For two-phase systems of the air-water, air-kerosene, etc. type the instability of the continuous profile is due to gradient flow of the denser liquid in the boundary layer and is described by the dispersion relation for the dimensionless "frequency"  $z = \omega\delta/V_i$  of a disturbance of the type  $\exp(ihx - i\omega t)$ ,

$$(z - \Delta)[(z - \Delta)(z + \Delta A) + \Delta(1 - A)] = (z - \Delta A) \left[ \alpha \Delta^3 We_b^{-1} - \frac{\Delta \delta g \cos \varphi}{V_i^2} \right], \quad (1)$$

where  $\Delta = h\delta$ ;  $A = (1 - \exp(-2\Delta))/2$ .

An analysis of the development of gradient instability under the conditions of the flow of a gas stream over a drop is of interest. Below we find the conditions for the appearance of instability, estimates of the main characteristics of the destruction are obtained, and certain conclusions about the character of the destruction are drawn on this basis.

First of all we must investigate the vicinity of the rim of the drop ( $\varphi = \pi/2$ ), where the separation of particles is observed experimentally. Here the influence of acceleration is

---

I. I. Mechnikov State University, Odessa. Translated from *Inzhenerno-Fizicheskii Zhurnal*, Vol. 48, No. 5, pp. 771-776, May, 1985. Original article submitted November 16, 1983.